

Urban Heat Island and Boundary Layer Structures under Hot Weather Synoptic Conditions: A Case Study of Suzhou City, China

ZHANG Ning^{*1} (张宁), ZHU Lianfang² (朱莲芳), and ZHU Yan² (朱焱)

¹*School of Atmospheric Sciences, Nanjing University, Nanjing 210093*

²*Suzhou Meteorological Bureau, Suzhou 215201*

(Received 8 July 2010; revised 19 October 2010)

ABSTRACT

A strong urban heat island (UHI) appeared in a hot weather episode in Suzhou City during the period from 25 July to 1 August 2007. This paper analyzes the urban heat island characteristics of Suzhou City under this hot weather episode. Both meteorological station observations and MODIS satellite observations show a strong urban heat island in this area. The maximum UHI intensity in this hot weather episode is 2.2°C, which is much greater than the summer average of 1.0°C in this year and the 37-year (from 1970 to 2006) average of 0.35°C. The Weather Research and Forecasting (WRF) model simulation results demonstrate that the rapid urbanization processes in this area will enhance the UHI in intensity, horizontal distribution, and vertical extension. The UHI spatial distribution expands as the urban size increases. The vertical extension of UHI in the afternoon increases about 50 m higher under the year 2006 urban land cover than that under the 1986 urban land cover. The conversion from rural land use to urban land type also strengthens the local lake-land breeze circulations in this area and modifies the vertical wind speed field.

Key words: urban heat island; hot weather; numerical simulation; urban boundary layer

Citation: Zhang, N., L. F. Zhu, and Y. Zhu, 2011: Urban heat island and boundary layer structures under hot weather synoptic conditions: A case study of Suzhou City, China. *Adv. Atmos. Sci.*, **28**(4), 855–865, doi: 10.1007/s00376-010-0040-1.

1. Introduction

Urbanization rapidly spreads all over the world, and the percentage of humans living in urban areas continues to grow worldwide. A study by the United Nations found that by 2050, 69.6% of the world's population will live in cities compared to 48.6% in 2005 and, in China, 72.9% of the total population will live in cities compared to 40.4% in 2005 (World Urbanization Prospects, United Nations, 2007, available at <http://esa.un.org/unup>).

The rapid urbanization process has created a critical issue facing the global society: the impact of urban environments on human health. Increased urbanization and environmental hazards lead to more direct and indirect weather-related accidents and deaths as well as significant economic loss (Changnon, 1992). For example, heat waves had devastating impacts in

Chicago in 1995 (Changnon, 1996; Semenza, 1996). Unfortunately, the frequency and intensity of heat waves will likely increase in the future (Meehl and Tebaldi, 2004), and urbanization may be one of the reasons causing heat wave increases over urban areas (Tan et al., 2008; Meng et al., 2010). Many cities have instituted heat watch warning technologies to mitigate impacts of heat waves (Ebi et al., 2004).

Urbanization changes surface radiation and dynamical features, modifies the heat and moisture exchange between the land surface and atmosphere, and then changes atmospheric properties above urban area, especially the planetary boundary layer (PBL) structure, by perturbing the wind, temperature, moisture, and turbulence. The urban heat island (UHI) phenomenon, characterized by a higher temperature contrast between a city and its surrounding rural areas, is one of the prominent urban effects. Roth and

*Corresponding author: ZHANG Ning, ningzhang@nju.edu.cn

Oke (1995) presented a comprehensive review of earlier observational studies on the characteristics, causes, and effects of UHI. Grimmond (2006) and Souch and Grimmond (2006) reviewed recent large campaign-style urban climate studies. These works have significantly advanced the recognition of spatial differences both within and between cities as a result of differences in urban fabric (materials and morphology), emissions, and prevailing meteorological and climatic conditions.

Typically, the UHI is greatest at night when temperatures measured within the city are warmer than rural temperatures. In addition, the magnitude of the UHI is dependent upon the location within a city. For example, the core of the city has more impact on the temperature than suburban areas due to the increased heat capacity of the man-made structures versus native vegetation (Martilli et al., 2002; Martilli, 2007). Zhang et al. (2005) reported that urbanization and other land cover change may contribute to the observed $0.12 \text{ K (10 yr)}^{-1}$ increase in the daily mean temperature, $0.20 \text{ K (10 yr)}^{-1}$ in the daily minimum temperature, and $0.03 \text{ K (10 yr)}^{-1}$ for the daily maximum surface temperature in China. Either high winds, clouds, or both disrupt the cooling differences between the urban and rural areas and reduce the UHI effect (Kidder and Essenwanger, 1995) while calm conditions with clear skies are optimal for large UHI effects (Lu et al., 1997a,b; Menut et al., 1999; Unger et al., 2001). The UHI is most noticeable at night and under synoptic high-pressure systems. Urban heat islands have been measured worldwide, such as in Mexico City (Oke et al., 1999), Tucson (Comrie, 2000), Phoenix (Fast et al., 2005), New York City (Childs and Raman, 2005; Gaffin et al., 2008), Beijing (Ji et al., 2006), and Shanghai (Chen et al., 2003). In addition, the UHI phenomenon has been observed for megacities as well as relatively small cities.

An urban heat island can also trigger mesoscale circulations (Urban Heat Island Circulations) when the UHI spatial size is big enough. Tang and Miao (1998) have simulated the UHI in the Yangtze River Delta and documented an interaction between UHI and UHI circulations. Wang (2009) compared the flow structures and turbulence characteristics of the UHI-induced mesoscale circulation over ideal urban areas by LES (large eddy simulations) modeling and demonstrated that the UHI spatial size has obvious influence on wind flow and turbulence features, especially under zero-wind conditions.

Urbanization converts the overlaying surface to urban covers made up of uprising buildings and increases the surface roughness over the urban area. The friction and drag of buildings will decrease the near-surface wind speed in the urban area. This aerodynamical

effect has been found by observations in many cities (e.g., Gao and Bian, 2004; Xu et al., 2009; Zhang et al., 2009). Miao et al. (2009a) simulated the influence of the morphological characteristics of buildings on the urban boundary layer structure of Beijing City with an urban boundary layer model. Zhang et al. (2010) documented that the urbanization may cause over 50% wind speed loss in Yangtze River Delta over the urbanized area, and such a wind speed decrease may happen not only over urban areas but on a regional scale.

In China, the urbanization process is accelerated with the rapid economical development. Urban heat islands have been reported in many cities, but most of the research has focused on megacities such as Beijing, Shanghai, etc. More studies are being carried out in many newly-developed cities, such as Suzhou, which play great roles in the Chinese urbanization processes and economical development. Rong et al. (2009) and Zhu and Zhu (2009) analyzed the urban heat island in Suzhou City from meteorological station observations and Landsat5 satellite observations and found that urban heat islands appear frequently over this area. The objectives of the present work are to quantify the intensity of the urban heat island of Suzhou City in a hot weather episode in the summer of 2007 using conventional observations and MODIS satellite sensing and to simulate the influences of land use change of urbanization on the UHI by using the WRF (Weather Research and Forecasting) model.

2. Research domain and synoptic background

2.1 Suzhou City

Suzhou City is located in the middle part of the Yangtze River Delta, which is one of the most developed and fast-developing areas in China (Fig. 1). Suzhou district is of a typical wet subtropical marine climate under the effect of the East Asia monsoon. The annual mean temperature of Suzhou district is about 17°C ; annual precipitation is about 1000 mm.

In the past 30 years, Suzhou City has experienced fast development with rapid urbanization. The population increased from 4.68 million in 1970 to 6.24 million in 2007, and the GDP (gross domestic product) increased from 1.5 billion Yuan in 1970 to 570 billion Yuan in 2007. The urban area also increased with such fast economical development. Figure 2 shows the urban built-up area of Suzhou City in 1986, 1995, and 2006 from Landsat5 satellite observations. This rapid urbanization process also enhances the urban heat island in this area.

2.2 Synoptic background

In late July and early August 2007, hot weather

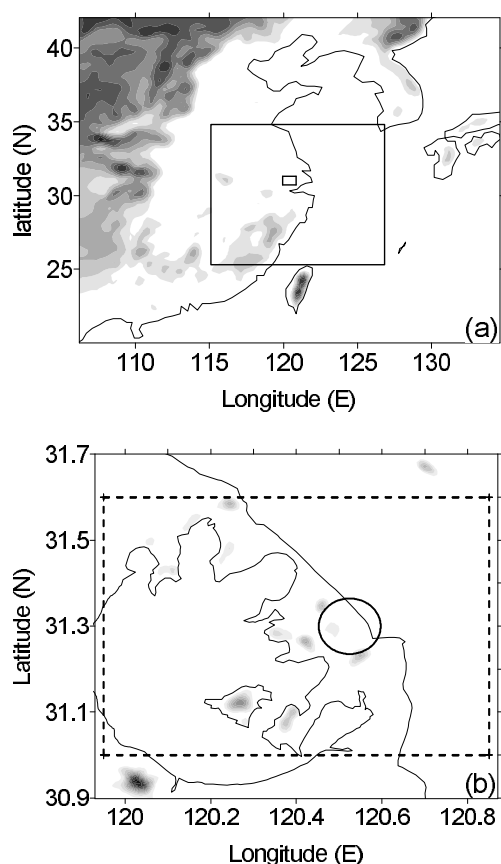


Fig. 1. Research domain and location of Suzhou City. (a) The nest configuration of the 3 nests WRF model simulation. (b) The inner domain of the WRF simulation, the land cover is the dot line box is updated with the Landsat satellite observations as shown in Fig. 2 and the circle indicating the location of Suzhou City.

occurred in Suzhou and lasted for about twenty days. The observed mean temperature of July 2007 was 30.3°C at Suzhou meteorological station while the mean temperature of July in a normal year is only 27.9°C ; in August, the monthly mean temperature of 2007 was 29.8°C compared to the monthly mean value of 27.6°C in a normal year. On 28 and 29 July and the first two days of August the observed maximum temperature at Suzhou station reached 39.3°C , which is the highest temperature observed historically.

This hot weather was caused by a continuous influence of a subtropical high-pressure zone. Figure 3 shows the 500 hPa synoptic background at 1200 LST 25 July 2007 and 1400 LST 1 August 2007 from the NCEP reanalysis data. This hot weather episode includes two typical synoptic conditions causing hot weather over the Yangtze River Delta. (1) In late July, the Yangtze River Delta was affected by a stable subtropical high, and a warm center (temperature $\geq -3^{\circ}\text{C}$ at the 500 hPa pressure level) appeared in

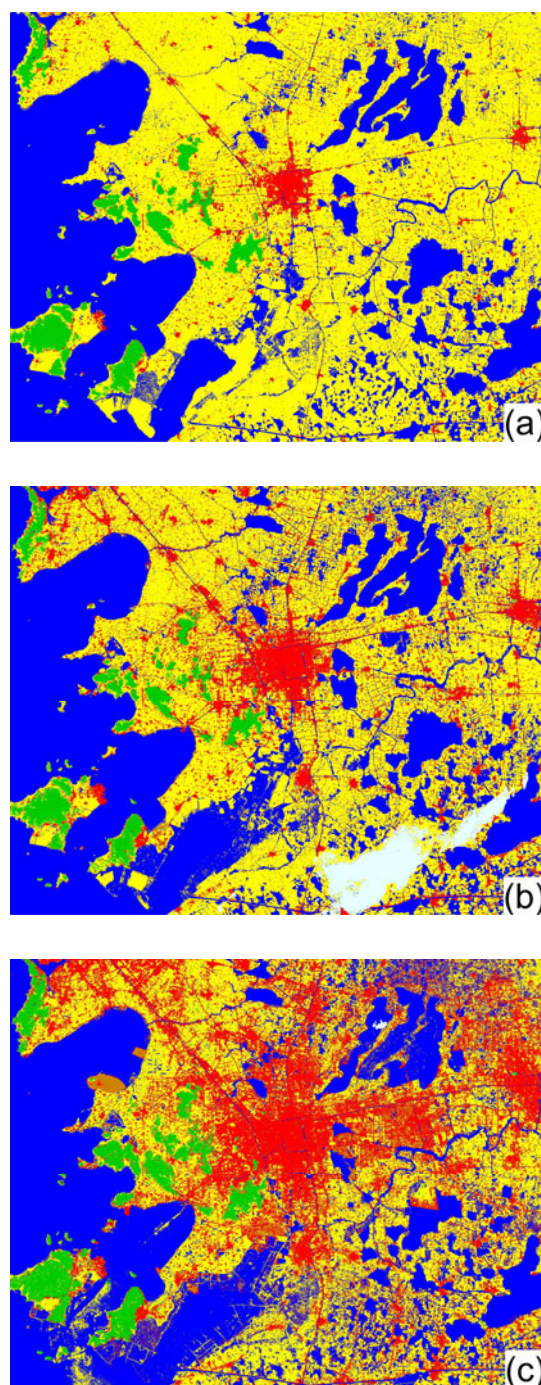


Fig. 2. Land cover change around Suzhou City in (a) 1986; (b) 1995, and (c) 2006 from Landsat5 observations (Red: urban built-up area; Green: forest; Blue: water; Yellow: farm land).

this area. (2) In early August the hot weather continued due to the effect of Typhoon Usagi. The subtropical high zone broke into two parts, and the western part controlled the Yangtze Delta. This made the hot weather continue.

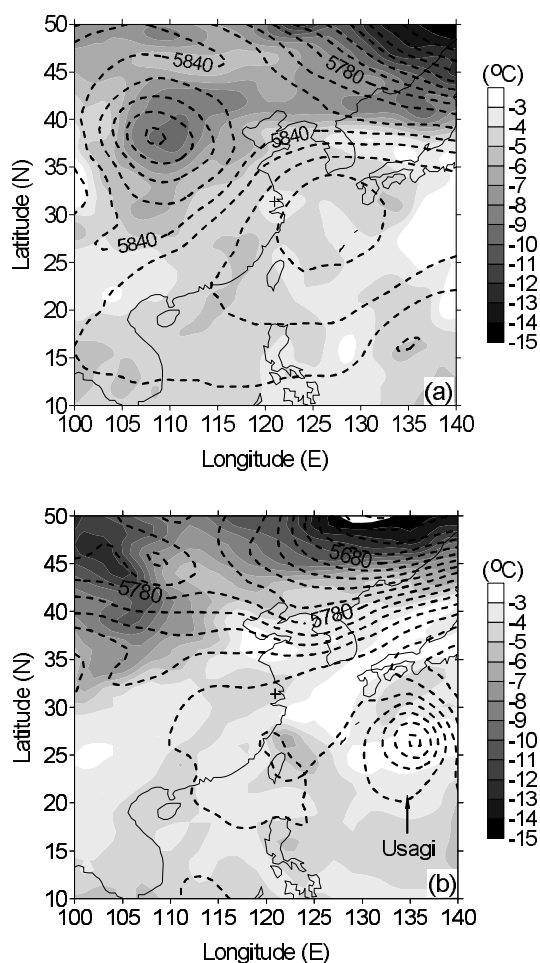


Fig. 3. Synoptic background condition at (a) 1400 LST 25 July 2007 and (b) 1400 LST 1 August 2007 from the NCEP reanalysis data. The dot contour lines show the geopotential at 500 hPa and the grey shadows show the temperature at 500 hPa.

3. Observed urban heat island intensity

3.1 UHI intensity diurnal change

Urban heat island intensity is usually defined as the near-surface air temperature difference between an urban area and rural area. For meteorological station observations, it is important to select reasonable stations to calculate the UHI intensity (Rong et al., 2009). Especially for historical UHI estimations, it is difficult to determine the real UHI intensity because there were always too few observations in urban areas. The annual mean near-surface temperature difference between Suzhou station (as the urban stations, this is nearest station to the Suzhou urban area which has long-term observations, but it is not good enough for representing the urban meteorological conditions) and Changshu and Kunshan stations (as the rural stations)

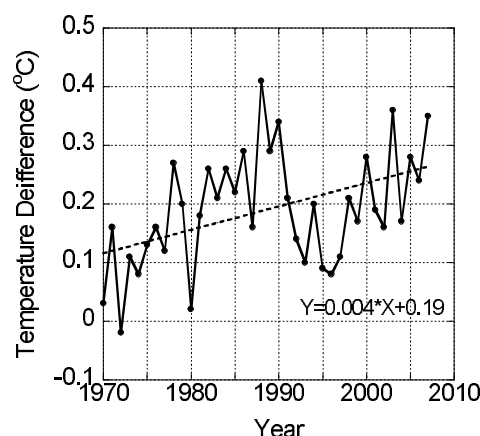


Fig. 4. Temperature difference at 2 m between Suzhou station and Kunshan, Changshu stations from 1970–2007.

from 1970 to 2007 is shown in Fig. 4. Even though the stations are not good enough for UHI monitoring, the temperature difference also has a weak but obvious increasing trend in the past 37 years with the urbanization processes in this area. The increasing ratio is about $0.004^{\circ}\text{C yr}^{-1}$. A sharply decrease in the temperature difference appeared near 1990; the possible reason is that the Changshu observation station relocated at that time due to a surrounding observation environment change. The analysis of 30-year long-term observations shows that the air temperature difference is very weak; it is only 0.1°C in the morning and 0.35°C in the afternoon (Fig. 5).

With the establishment of the automatic meteorological observation network in Suzhou City since the year 2007, more and more automated meteorological stations have been built in the Suzhou urban area (the locations of meteorological stations are shown in Fig. 6). These stations supply more and better observations in the urban area. In this paper, the UHI is defined as the temperature difference between all station observations in the urban area (as shown in Fig. 2c) and other stations. As mentioned above, the urban heat island is more obvious under clear-sky conditions. In this hot weather episode (25 July to 5 August 2007), a strong urban heat island was also observed in the Suzhou region. Due to the rapid urbanization process and more observations in urban area, the UHI intensity in the summer of 2007 is stronger than the 37-yr average temperature difference between Suzhou station and Changshu and Kunshan stations. In this hot weather episode, the UHI is much stronger than the whole summer averages of the year 2007, and the UHI intensity has a much greater diurnal range. The UHI intensity in this hot weather episode varies from 0.1°C to 2.2°C compared to 0.4°C to 1.0°C for the

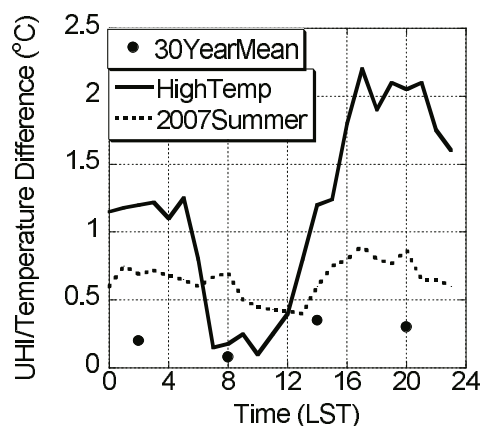


Fig. 5. Diurnal variation of urban heat intensity (UHI) intensity. The dots are mean values of 30 years from 1977 to 2007; the solid line (HighTemp: high temperature) and the dot line (2007Summer: summer of 2007) are mean values of air temperature difference between urban and rural stations for 182 days (June, July, August 2007) and ten days (from 25 July to 5 August 2007) in this hot weather scenario.

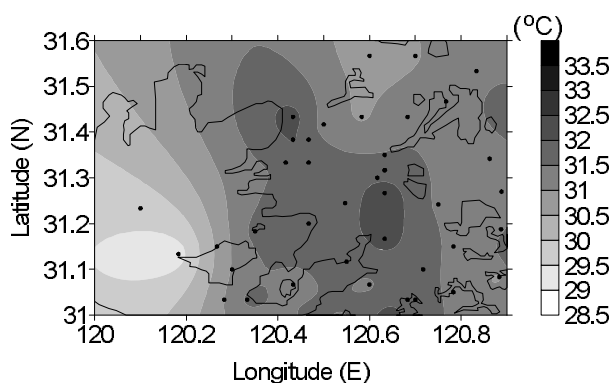


Fig. 6. Averaged spatial distribution of observed UHI in 25 July to 5 August 2007 from conventional and automatic meteorological stations (the dots indicating the station locations).

whole summer average. In the hot weather episode, the mean UHI intensity is 1.2°C , the maximum is 2.2°C , the minimum is 0.1°C , and the daily deviation is 0.7°C . For the whole summer average in 2007, the mean intensity UHI is 0.7°C , the maximum is 1.0°C , the minimum is 0.4°C and the daily deviation is 0.15°C .

Both the diurnal changes of UHI intensity in this hot weather episode and the mean diurnal changes in summer 2007 have similar variation trends. The maxima appear in the late afternoon, and the weakest UHIs appear in the early morning. The second peaks appear just before the sunrise (about 0500 LST).

3.2 UHI spatial distribution

Figure 6 shows the averaged near-surface temperature (temperature at 2 m) of this hot weather episode. The data are from 41 meteorological stations in the area, and the locations are shown as dots. The near-surface temperature field has a warm center at the city center of Suzhou, and temperature decreases in the rural areas. The average temperatures at urban observation stations are above 33°C ; the observations at rural stations are about 29°C – 31°C . The lowest temperature, appearing at Dongshan station near Lake Tai, is only about 28.5°C . The UHI high center also appeared in the city center of Suzhou. The mean UHI intensity over the domain is 1.1°C , the maximum UHI is 2.2°C , and the spatial deviation of UHI is 0.6°C .

The observed land surface temperature from the MODIS satellite also shows warmer centers over the urban area. Figure 7 illustrates the averaged MODIS observed surface temperature in daytime during this hot weather episode (In this period, only daytime MODIS observations are available). The distributions of MODIS surface temperature are very close to the urban built-up area distribution as shown in Fig. 2. The maximum surface temperature appeared at the center of Suzhou City and was above 45°C . The surface skin temperatures over rural areas were 35°C – 30°C and the surface skin temperatures over water areas were below 33°C . The UHI distribution had a similar trend to the surface skin temperature distribution. The maximum departure of 5.6°C appears in the city center of 5.6°C ; the spatial deviation of surface temperature departure is 2.9°C .

The spatial distributions of both the UHI and the surface temperature departures have peaks in the concentrated urban built-up area; the high value zones distribute north-west to south-east as the urban area

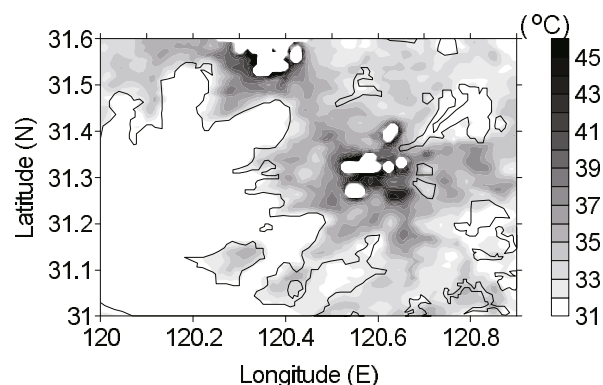


Fig. 7. MODIS observed averaged daytime surface skin temperature from 25 July to 5 August 2007 (blank indicating missing values).

Table 1. Configurations of the physical parameterization schemes in WRF.

Physical Processes	Parameterization Scheme
Planetary boundary layer process	Mellor Yamada Jajic turbulence kinetic energy scheme
Land-surface process	NOAH land surface model (*)
Long-wave radiation	RRTM long wave radiation scheme
Shortwave radiation	Simple shortwave radiation scheme
Microphysics	Lin microphysics scheme
Surface layer	Eta
Convection	Kain-Fritsch (new Eta) (**)

Note: (*) Original NOAH land surface model without urban canopy model for the 21 km resolution nest and NOAH land surface model coupled urban canopy schemes for the 3-km resolution nest and the 1-km resolution nest. (**) Convection scheme is only used for the 21 km resolution nest.

Table 2. Comparison between meteorological station observations and WRF simulations.

	OBS	1986		1995		2006	
		SIM	RMSE	SIM	RMSE	SIM	RMSE
Air temperature at 2 m ($^{\circ}\text{C}$)	32.8	30.3	2.5	30.4	2.5	32.6	0.5
Specific humidity at 2 m (g kg^{-1})	19.0	20.7	1.8	20.8	2.0	18.5	0.9
Wind speed at 10 m (m s^{-1})	1.7	2.0	1.1	1.9	0.8	1.5	0.3

distributes. Both meteorological station observations and MODIS satellite observations indicate that more hot weather may occur in urban centers in this hot weather episode.

4. WRF simulated urbanization influence on urban meteorological conditions

4.1 Case design

The results in section 3 show that a strong UHI appears in the urban area during this hot weather episode, meaning that the air temperature over the urban area is much higher than that over rural area. Suzhou City has experienced a rapid urbanization process in the last 20 years as shown in Fig. 2. This will enhance the urban heat island and may increase the negative consequences. In this section, a WRF model is used to simulate the hot weather episode using different urbanization statuses in 1986, 1995, and 2006 from the LandSat5 satellite observations to study the influence of urbanization on the local meteorological environment.

The WRF model is configured as three nested runs over this area. The model domains are shown in Fig. 1. All nests are of 101×101 grids, with resolutions of $21 \text{ km} \times 21 \text{ km}$, $3 \text{ km} \times 3 \text{ km}$, and $1 \text{ km} \times 1 \text{ km}$, respectively. NCEP $1^{\circ} \times 1^{\circ}$ reanalysis data are used to initialize and support lateral boundary conditions for the 21 km nest. A single layer urban canopy scheme coupled in the NOAH (National Centers for Environmental Prediction -Oregon State University - Air Force -Hydrologic Research Lab) land surface model is used

to present the influence of the urban surface. The parameterization schemes used in our simulation are listed in Table 1, including long-wave/short-wave radiation processes, planetary boundary layer process, land surface processes, microphysical processes, and so on. In the WRF model, a single-layer urban canopy model was implemented in the NOAH land surface model to represent the thermal and dynamic effects of urban buildings, including trapping radiation within the urban canopy: after being reflected by roads and building walls, incoming direct radiation can be absorbed and/or reflected again by roads and wall surfaces. The model includes parameterization of the limited surface evaporation from impervious urban surfaces.

4.2 WRF simulations results

The WRF simulation results were first compared with the meteorological station observations in this area. There are 39 available stations for this comparison, including automatic weather stations and conventional meteorological stations. The station locations are illustrated in Fig. 6. The comparisons are shown in Table 2. For the 2006 cases, the error between simulations and observations and the RMSE, respectively, are 0.2°C and 0.5°C for near-surface temperature, 0.5 g kg^{-1} and 0.9 g kg^{-1} for near-surface specific humidity, and 0.2 m s^{-1} and 0.3 m s^{-1} for surface wind speed. The simulation errors and RMSEs in the 1986 and 1995 cases are much greater than those in the 2006 case. The WRF simulations prove that the WRF model can simulate this hot weather episode well, and

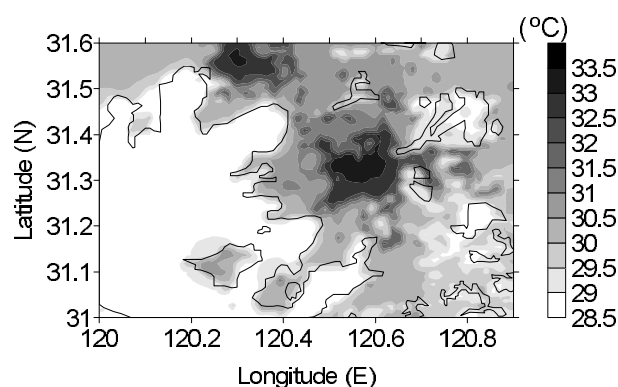


Fig. 8. WRF simulated averaged air temperature at 2 m from 25 July to 5 August 2007.

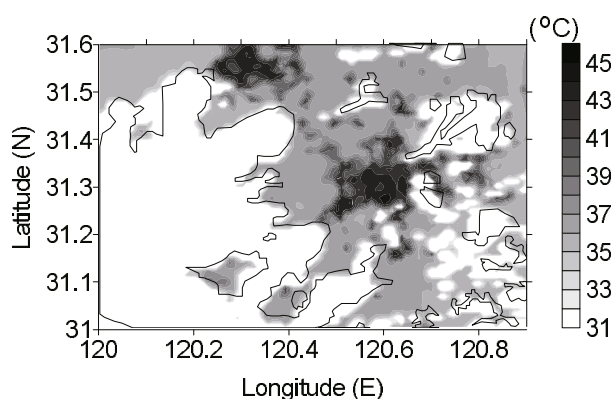


Fig. 9. WRF simulated averaged daytime surface skin temperature from 25 July to 5 August 2007.

the results from different cases also indicate that the improvement in land surface information can help improve the simulation results in the WRF model. Figures 8 and 9 show the average distribution of near-surface temperature and surface skin temperature in the 2006 case, respectively. The WRF simulations illustrated the southeast-northwest high value distribution of both temperature and surface temperature. The maximum near-surface temperature in the 2006 case appeared in the city center of Suzhou with a value of 33.4°C and a standard deviation of 1.18°C. The maximum surface skin temperature in the 2006 case also appeared in the city center of Suzhou with a value of 44.3°C and a standard deviation of 5.1°C. This indicates that the WRF model can represent this hot weather episode well with the 2006 land use cover.

The urbanization influences the near-surface temperature both in daytime and at night. For example, at 1500 LST on 1 August in the 1986 case, the maximum temperature is 38.7°C, the mean temperature over the land area is 36.1°C (Fig. 8), and the stan-

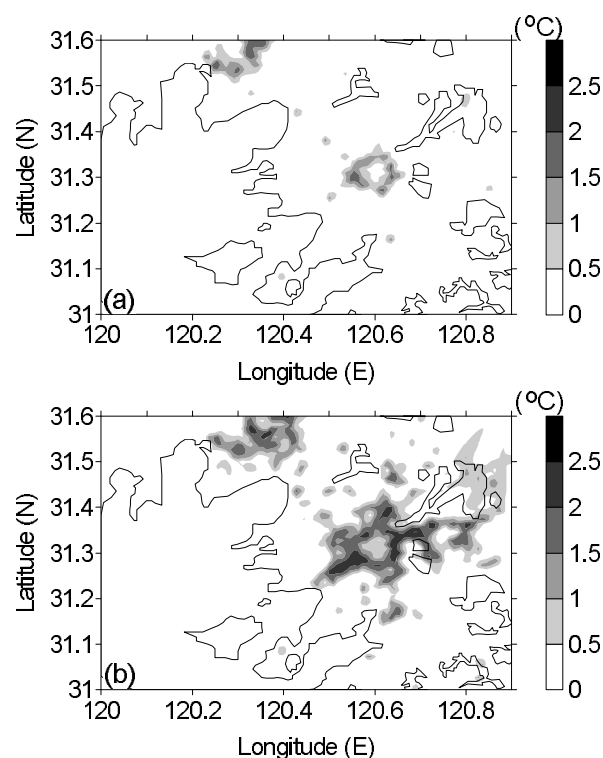


Fig. 10. WRF simulated T2 difference at 1500 LST 1 August: (a) case 1986 minus case 1995; (b) case 2006 minus case 1986.

dard deviation is 0.8°C. In the 1995 case, the maximum is 39.1°C, the mean is 36.2°C, and the standard deviation is 0.9°C. In the 2006 case, the maximum is 39.4°C, the mean is 36.5°C, and the standard deviation is 1.1°C. At 1800 LST on 1 August 1986, the maximum temperature is 29.7°C, the mean temperature over the land area in Fig. 7 is 26.1°C, and the standard deviation is 0.7°C. In the 1995 case, the maximum is 30.4°C, the mean is 26.2°C, and the standard deviation is 0.8°C. In the 2006 case, the maximum is 30.2°C, the mean is 26.7°C, and the standard deviation is 1.1°C. The urbanization also enhance the UHI intensity at the same time. Figures 10 and 11 illustrate the differences of near-surface temperature and surface skin temperature between the 1986 and 1995 cases and between the 1986 and 2006 cases at 1500 LST on 1 August. The UHI intensity increases about 2.5°C in the newly urbanized area, and the surface skin temperature increases about 10°C. The influence on surface skin temperature is directly related to the expanding of urban land cover size. Where urbanization converts land cover to urban land use, the surface skin temperature will increase, and the area over which surface skin temperature increase is about the same size of the urbanized area. Near-surface temperature increases in a wider area than the urbanization.

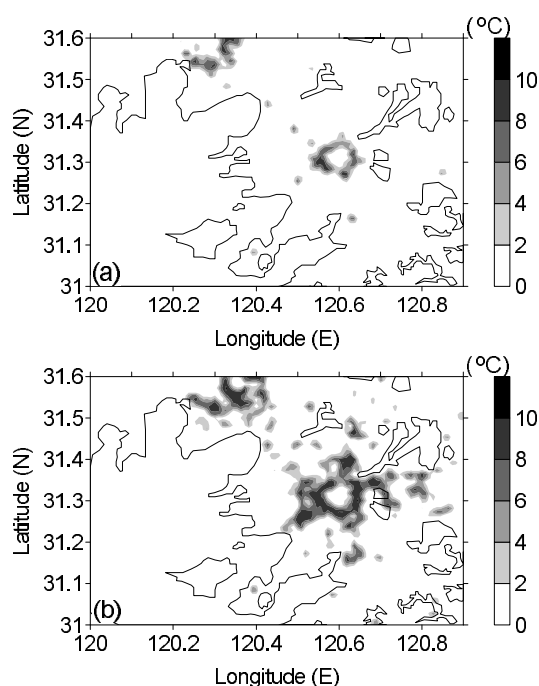


Fig. 11. WRF simulated TSK difference at 1500 LST 1 August: (a) case 1986 minus case 1995; (b) case 2006 minus case 1986.

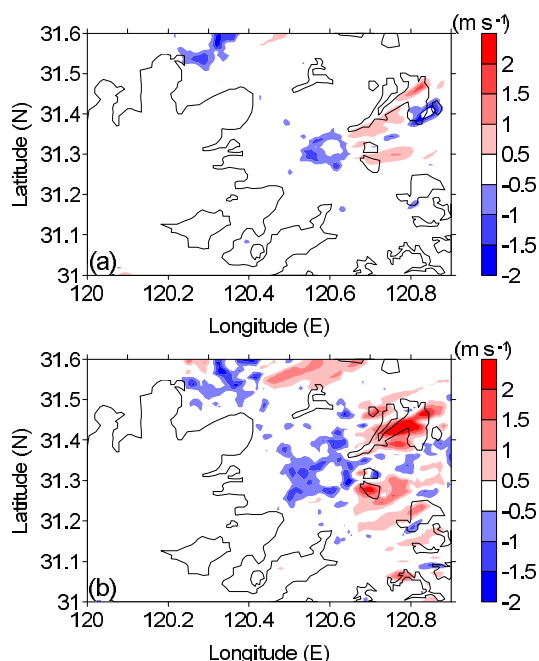


Fig. 12. WRF simulated wind speed difference at 1500 LST 1 August: (a) case 1986 minus case 1995; (b) case 2006 minus case 1986.

For example, in Fig. 11, no surface skin temperature increase happened in the old city area (the urban area

in 1986) compared with results of the 1995 case and the 2006 case, while there is an increase in near-surface temperature in the core of the urban area in the 1995 and 2006 cases because of the background wind advection. The near-surface temperature increase is also obvious in the windward area beyond Suzhou City in the 1995 and 2006 cases due to the strong background wind conditions. Zhang et al. (2010) also documented that the temperature increases caused by urbanization might appear on a regional scale in the Yangtze River Delta.

The urbanization also changes the surface aerodynamic characteristics. The building clusters in urban areas will increase the local roughness and reduce the surface wind speed. Figure 12 shows the near-surface wind speed differences between the 1986 and 1995 cases and difference between the 1986 and 2006 cases. The wind speed lost in the urban area is about 2 m s^{-1} in these simulations, and the wind speed loss area is very close to the land surface change caused by the urbanization. It is interesting to note that urbanization will enhance the wind speed over the water surface in the windward direction of the urban area.

Figures 13 and 14 show the diurnal cycle of surface temperature, surface skin temperature, and surface energy balance over the urban area (the red shadowed area in Fig. 2c) in the 1986, 1995, and 2006 cases. In our simulations, the net radiation over the urban area does not change much in the urbanization processes, but the surface energy partition changes greatly. In the urbanization processes, the underlying surface is modified to a waterproof surface made up of cement and other building materials. This reduced the available surface soil moisture and impacted the heat flux partitions in the urbanized areas with an increase in sensible heat flux and decrease in latent heat flux. In the simulations for this paper, urbanization also changed the surface energy balance in this area. For example, in the 1986 case, the average surface sensible heat flux is 180 W m^{-2} , the average latent heat flux is 405 W m^{-2} at noon (1200 LST), and the Bowen ratio is 0.44. In the 1995 case, the sensible heat flux is 207 W m^{-2} , the latent heat flux is 380 W m^{-2} , and the Bowen ratio is 0.54. In the 2006 case, the sensible heat flux is 311 W m^{-2} , the latent heat flux is 178 W m^{-2} , and the Bowen ratio is 1.75. The surface heat flux partitioning over the urbanized area changed from latent heat flux dominance to sensible heat flux dominance. This phenomenon is also found by Trusilova et al. (2008), Miao et al. (2009b), and Zhang et al. (2010).

Because of the great land-water difference, a “warm island” appears over the land area in the daylight time, and the urban heat island caused by the urbanization

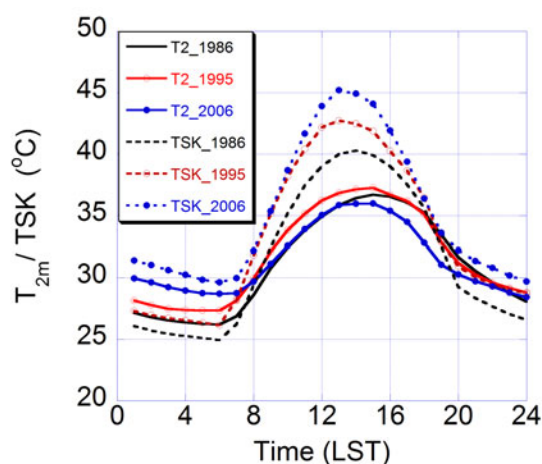


Fig. 13. WRF simulated diurnal variations of near-surface temperature and surface skin temperature over urban area in case 2006 in different cases.

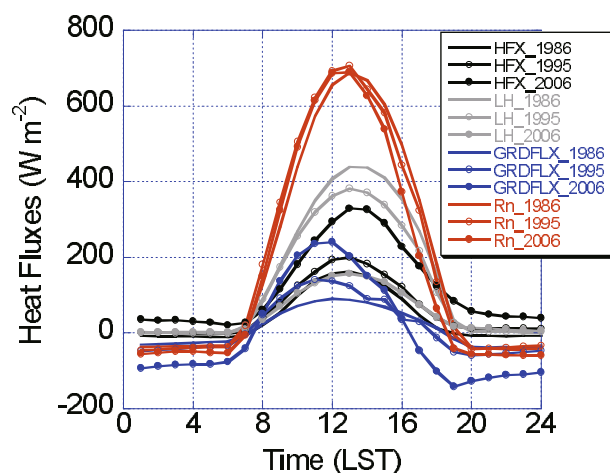


Fig. 14. WRF simulated diurnal variations of surface energy balance over urban area in case 2006 in different cases.

process will strengthen the “warm island” over land and enhance its vertical extension. For example, at 1400 LST 1 August 2007, a warm heat island appears in all cases: the maximum height of the 34°C contour line increased from 336 m in the 1986 case to 360 m in the 1995 case and 389 m in the 2006 case.

Lake-breeze circulation may be triggered by the temperature difference between the land area and water surface. For the cities near sea or lake, the interaction between the sea/lake-breeze and UHI circulation is very complicated. Lemonsu et al. (2006) documented that the urban effects appear to be negligible under strong a sea-breeze front, while Freitas et al. (2007) found that a UHI may form a strong convergence zone in the center of the city and, thereby, acce-

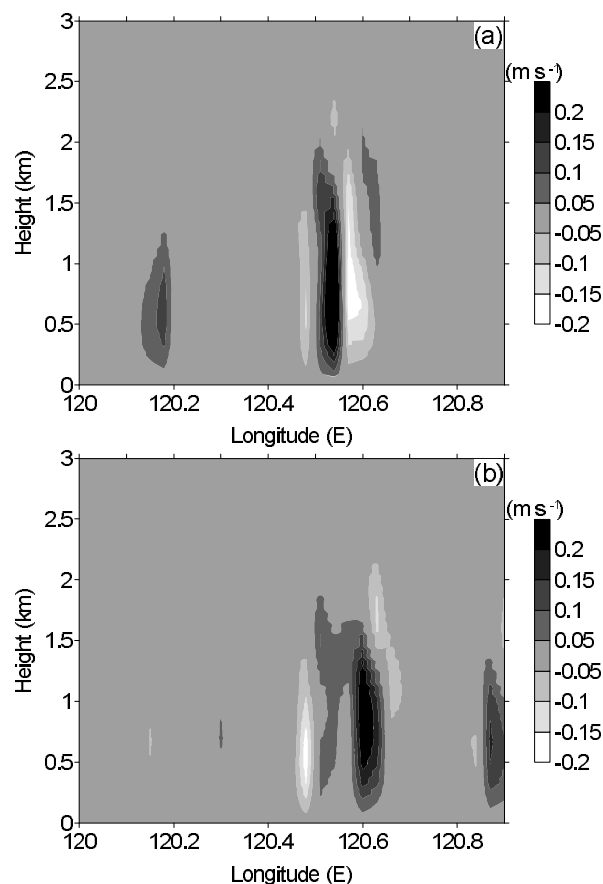


Fig. 15. WRF simulated vertical wind speed difference cross Suzhou City (through the section of 32.3°N) at 1500 LST 1 August: (a) case 1986 minus case 1995; (b) case 2006 minus case 1986.

lerate the sea-breeze front toward the center of the city. In our simulations, neither complete lake-breeze circulation nor UHI circulation appeared due to the strong ambient west wind (horizontal average is about 8.0–10.0 m s⁻¹ at 10 m), but the results still indicate that urbanization also enhances the land-lake breeze circulation when it strengthens the urban heat island. Figure 15 shows the west-east vertical section of vertical wind speed difference along 32.3°N (crossing the center of Suzhou City) at 1400 LST 1 August 2007. The upward wind speed increased with the urban area expansion in the Suzhou area. The vertical wind speed difference between the 1986 case and the 1995 case shows that over the newly built urban area, upward wind is strengthened nearly 0.1 m s⁻¹ with a peak value of 0.2 m s⁻¹ at the height of 700 m, while over the area on the leeward side of the urban area, downward wind speed strengthened by about 0.15 m s⁻¹. In the windward area, downward wind speed also strengthened by about 0.05 m s⁻¹ before reaching the urban area. In the 2006 case, the upward wind speed also

strengthened over the urban area, and the downward wind strengthened by about 0.15 m s^{-1} before the urban area. At the same time, the downward wind was weakened due to the urban expanding in this direction, and a new upward wind center appeared at the location of 120.9°E , where a dense new urban center appeared.

5. Summary

The urban heat island characteristics of Suzhou City under a hot weather episode from 25 July to 1 August 2007 are analyzed in this paper. Both meteorological station observations and MODIS satellite observations show a strong urban heat island in this area. The UHI has a similar daily variation in this hot weather episode to the whole summer average but a much stronger intensity. The maximum UHI appears in the afternoon. The maximum UHI intensity is 2.2°C , which is much greater than the summer average of 1.0°C in this year and the 30-year average of 0.35°C . The WRF simulation results demonstrate that the rapid urbanization processes in this area will enhance the UHI in intensity, horizontal area, and vertical extension. The UHI spatial distribution expands as the urban land cover increases. The vertical extension of the UHI in the afternoon increases to about 50 m higher under the year 2006 urban land cover than that under the 1986 urban land cover. The conversion from rural land use to urban land type also strengthens the local lake-land breeze circulations in this area and modifies the vertical wind speed field.

Acknowledgements. This paper is sponsored by the National Basic Research Program of China (2010CB428501 and 2011CB952002) and National Natural Science Foundation of China (Grant No. 41005008).

REFERENCES

- Changnon, S. A., 1992: Inadvertent weather-modification in urban areas: Lessons for global climate change. *Bull. Amer. Meteor. Soc.*, **73**, 619–627.
- Changnon, S. A., K. E. Kunkel, and B. C., Reinke, 1996: Impacts and responses to the 1995 heat wave: A call to action. *Bull. Amer. Meteor. Soc.*, **77**, 1497–1506.
- Childs, P. P., and S. Raman, 2005: Observations and numerical simulations of urban heat island and sea breeze circulations over New York City. *Pure Appl. Geophys.*, **162**, 1955–1980.
- Chen, L., W. Zhu, X. Zhou, and Z. Zhou, 2003: Characteristics of the heat island effect in Shanghai and its possible mechanism. *Adv. Atmos. Sci.*, **20**, 991–1001.
- Comrie, A. C., 2000: Mapping a wind-modified urban heat island in Tucson, Arizona (with comments on integrating research and undergraduate learning). *Bull. Amer. Meteor. Soc.*, **81**, 2417–2431.
- Ebi, K. L., T. J. Teisberg, L. S. Kalkstein, L. Robinson, and R. F. Weiher, 2004: Heat watch/warning systems save lives—Estimated costs and benefits for Philadelphia 1995–98. *Bull. Amer. Meteor. Soc.*, **85**, 1067–1073.
- Fast, J. D., J. C. Torcolini, and R. Redman, 2005: Pseudo-vertical temperature profiles and the urban heat island measured by a temperature datalogger network in Phoenix, Arizona. *J. Appl. Meteor.*, **44**, 3–13.
- Freitas, E. D., C. M. Rozoff, W. R. Cotton, and P. L. S. Dias, 2007: Interactions of an urban heat island and sea-breeze circulations during winter over the metropolitan area of Sao Paulo, Brazil. *Bound.-Layer Meteor.*, **122**(1), 43–65.
- Gaffin, S. R., and Coauthors, 2008: Variations in New York city's urban heat island strength over time and space. *Theor. Appl. Climatol.*, **94**, 1–11.
- Gao, Z., and L. Bian, 2004: Estimation of aerodynamic roughness length and displacement of an urban surface from single-level sonic anemometer data. *Aust. Meteor. Mag.*, **54**, 21–28.
- Grimmond, C. S. B., 2006: Progress in measuring and observing the urban atmosphere. *Theor. Appl. Climatol.*, **84**, 3–22.
- Ji, C. P., W. D. Liu, and C. Y. Xuan, 2006: Impact of urban growth on the heat island in Beijing. *Chinese J. Geophys.*, **49**(1), 69–77. (in Chinese)
- Kidder, S. Q., and O. M. Essenwanger, 1995: The effect of clouds and wind on the difference in nocturnal cooling rates between urban and rural-areas. *J. Appl. Meteor.*, **34**, 2440–2448.
- Lemonsu, A., S. Bastin, V. Masson, and P. Drobinski, 2006: Vertical structure of the urban boundary layer over Marseille under sea-breeze conditions. *Bound.-Layer Meteor.*, **118**(3), 477–501.
- Lu, J., S. P. Arya, W. H. Snyder, and R. E. Lawson, 1997a: A laboratory study of the urban heat island in a calm and stably stratified environment. 1. Temperature field. *J. Appl. Meteor.*, **36**, 1377–1391.
- Lu, J., S. P. Arya, W. H. Snyder, and R. E. Lawson, 1997b: A laboratory study of the urban heat island in a calm and stably stratified environment. 2. Velocity field. *J. Appl. Meteor.*, **36**, 1392–1402.
- Martilli, A., 2007: Current research and future challenges in urban mesoscale modelling. *International Journal of Climatology*, **27**, 1909–1918.
- Martilli, A., A. Clappier, and M. W. Rotach, 2002: An urban surface exchange parameterisation for mesoscale models. *Bound.-Layer Meteor.*, **104**, 261–304.
- Meehl, G. A., and C. Tebaldi, 2004: More intense, more frequent, and longer lasting heat waves in the 21st century. *Science*, **305**, 994–997.
- Meng, W., Y. Zhang, J. Li, W. Lin, G. Dai, and H. Li, 2010: Application of WRF/UCM in the simulation of a heat wave event and urban heat island around Guangzhou city. *Journal of Tropical Meteorology*, **26**, 273–282. (in Chinese)
- Menut, L., C. Flamant, and J. Pelon, 1999: Evidence of

- interaction between synoptic and local scales in the surface layer over the Paris area. *Bound.-Layer Meteor.*, **93**, 269–286.
- Miao, S., P. Li., and X. Wang, 2009a: Building morphological characteristics and their effect on the wind in Beijing. *Adv. Atmos. Sci.*, **26**(6), 1115–1124, doi: 10.1007/s00376-009-7223-7.
- Miao, S. G., F. Chen, A. L. Magaret, T. Mukul, Q. Li, and Y. Wang, 2009b: An observational and modeling study of characteristics of urban heat island and boundary layer structures in Beijing. *J. Appl. Meteor. Climatol.*, **48**(3), 484–501.
- Oke, T. R., R. A. Spronken-Smith, E. Jauregui, and C. S. B. Grimmond, 1999: The energy balance of central Mexico City during the dry season. *Atmos. Environ.*, **33**, 3919–3930.
- Rong, C., H. Liu, and Y. Zhu, 2009: The study of the urban heat island and its influence factors in Suzhou City. *Scientia Meteorologica Sinica*, **29**(1), 84–87.
- Roth, M., and T. R. Oke, 1995: Relative efficiencies of turbulent transfer of heat, mass, and momentum over a patchy urban surface. *J. Atmos. Sci.*, **52**, 1863–1874.
- Semenza, J. C., 1996: Deaths in the Chicago heat wave. *New England Journal of Medicine*, **335**, 1848–1849.
- Souch, C., and S. Grimmond, 2006: Applied climatology: Urban climate. *Progr. Phys. Geogr.*, **30**, 270–279.
- Tan, J., Y. Zheng, G. Pen, S. Gu, and J. Shi, 2008: Effect of urban heat island on heat waves in summer of Shanghai. *Plateau Meteorology*, **27**, 144–149. (in Chinese)
- Tang, Y., and M. Miao, 1998: Numerical studies on urban heat island associated with urbanization in Yangtze Delta region. *Adv. Atmos. Sci.*, **15**(3), 393–403.
- Trusilova, K., M. Jung, G. Churkina, U. Karstens, M. Heimann, and M. Claussen, 2008: Urbanization impacts on the climate in Europe: Numerical experiments by the PSU-NCAR Mesoscale Model (MM5). *J. Appl. Meteor. Climatol.*, **47**(5), 1442–1455.
- Unger, J., Z. Sumeghy, A. Gulyas, Z. Bottyan, and L. Mucsi, 2001: Land-use and meteorological aspects of the urban heat island. *Meteorol. Appl.*, **8**, 189–194.
- Wang, W. G., 2009: The influence of thermally-induced mesoscale circulations on turbulence statistics over an idealized urban area under a zero background wind. *Bound. Layer Meteor.*, **131**(3), 403–423.
- Xu, Y., S. Liu, F. Hu, N. Ma, Y. Wang, Y. Shi, and H. Jia, 2009: Influence of Beijing urbanization on the characteristics of atmospheric boundary layer. *Chinese J. Atmos. Sci.*, **33**(4), 859–867. (in Chinese)
- Zhang, J., W. Dong, L. Wu, J. Wei, P. Chen, and D. Lee, 2005: Impact of land use changes on surface warming in China. *Adv. Atmos. Sci.*, **22**, 343–348.
- Zhang, N., W. Jiang, Z. Gao, F. Hu, and Z. Peng, 2009: Determination of urban surface aerodynamic characteristics using Marquardt method. *Wind and Structures*, **12**(3), 281–283.
- Zhang, N., Z. Gao, X. Wang, and Y. Chen, 2010: Modeling the impact of urbanization on the local and regional climate in Yangtze River Delta, China. *Theor. Appl. Climatol.*, **102**, 331–342.
- Zhu, Y., and L. Zhu, 2009: An analysis on summer urban heat island in Suzhou using satellite data. *Scientia Meteorologica Sinica*, **29**(1), 77–83.